

Intraparticle structures of composite TiO₂/SiO₂ nanoparticles prepared by varying precursor mixing modes in vapor phase

W.-H. CHO, D.-J. KANG, S.-G. KIM

Department of Chemical Engineering, Chung Ang University, 221, Huksuk-Dong, Dongjak-Ku, Seoul, 156-756, Korea

E-mail: sgkim@cau.ac.kr

TiO₂-SiO₂ composite nanoparticles with different intraparticle structures were prepared by varying modes of reactant mixing in equimolar vapor-phase hydrolysis of TTIP and TEOS. They included the structures of core-shell, either titania core surrounded by silica shell (abbreviated by T-S) or vice versa (S-T), and of mixed type, one oxide dispersed in the other (T/S). Design of mixing junction between TTIP and H₂O was very critical due to high hydrolysis rate of TTIP. That of TEOS was, however, so low that atomic silicon percentage of the particles was always less than 50%. The percentage increased with the temperature of reactor and the free surface of titania. Thus, due to the availability of the surface, the highest and the smallest silicon contents were obtained in the T/S and the S-T particles, respectively. In case of the former, as the temperature increased to 950°C, the silicon content reached 50% and, moreover, silica-rich particles appeared originating from homogeneous nucleation of the component. Average size of primary particles, irrespective of the structures, decreased with the content of silicon. In addition to the silicon effect, the gap in the sizes of the T-S and the S-T particles was further promoted, ultimately by the difference in the hydrolysis rates of the two alkoxides. The difference also caused radial gradient of composition even inside each primary T/S particle. Structural identity of shell component was affected by the existence of core component for both the T-S and the S-T particles. © 2003 Kluwer Academic Publishers

Introduction

Nanosized titania (TiO₂) particles, as in either pure or composite form, have been enormously used in white pigments, catalysts, catalyst supports, ceramic membranes, fiber optics, varistors, capacitors and so on [1]. In order to reveal various functionalities of the particles, it is very important to carefully control their intraparticle properties, such as size, morphology, crystalline phase, chemical composition and structure of the composites [2]. For laboratory-scale production of the TiO₂ particles, chemical vapor condensation (CVC) reactors have been widely used due to their simplicity, versatility and controllability, where mostly titanium chloride vapor reacts with oxygen well above 1000°C [3–5]. The effect of water vapor in the oxidation of titanium chloride was discussed in the literatures [3, 4]. They showed that the presence of water vapor resulted in more rounded primary particles with smaller sizes. Recently, however, the reaction temperature has been lowered as low as 250°C and 110°C by using thermal decomposition [6, 7] and hydrolysis [8, 9] of titanium tetraisopropoxide (TTIP), respectively. The hydrolysis of the titanium alkoxide has been known to simultaneously accompany the decomposition of the precursor in the ordinary CVC reactors. Kirkbir *et al.* [9] discussed

relative importance of the two reactions to conclude that higher water vapor concentration and lower reactor temperature favored the hydrolysis. To enhance the characteristics of the particles, SiO₂ has been added to them as shell, core [10–12] or in a dispersed phase [13–15] since the component introduced plays a role of controlling the photocatalytic activities and the refractive indices, and raising the compatibilities of the particle surface when dispersed in liquid or solid matrices. Furthermore, the composite particles even showed the synergetic effect of the composites such as the generation of new catalytic active sites due to the interaction of TiO₂ with SiO₂ [16]. TiO₂-SiO₂ composite particles were also prepared mostly by oxidation of vapor of the corresponding chlorides. Suyama *et al.* [13] and Ehrman *et al.* [12] suggested that Si⁴⁺ is small enough to enter TiO₂ lattice interstitially and thus SiO₂ inhibits growth of the primary particles as well as their anatase-to-rutile transformation. We found some possibility of producing the same composite structures as above simply by changing the methods of precursor mixing in our previous study on the hydrolysis of the corresponding alkoxides [17]. In present study, we varied the modes of precursor mixing more systematically under conditions controlled more precisely. We investigated effects

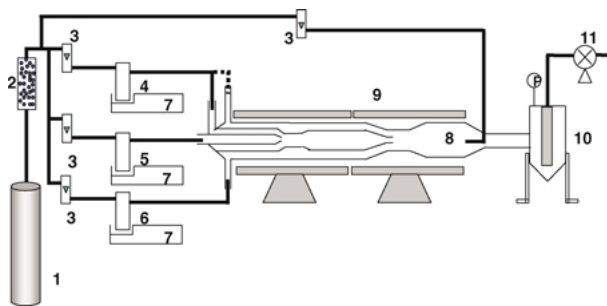


Figure 1 Experimental apparatus. 1. N₂ Gas, 2. Silica gel, 3. Flow meter, 4. TTIP, 5. H₂O, 6. TEOS, 7. Ultrasonic nebulizer, 8. Reactor, 9. Electrical furnace, 10. Bag filter and 11. Vacuum pump.

of the mixing modes on structure, size, bulk and surface compositions, and crystallinities of the primary particles composed of the two oxides.

Experimental

Fig. 1 shows schematic diagram of particle generation system used in this study. Nitrogen gas was sent through a series of drying columns containing silica gel and sulfuric acid, respectively. Then it passed three parallel ultrasonic nebulizers, all kept cool by circulating water at 25°C, which atomized reagent-grade titanium tetraisopropoxide (TTIP), Ti(OC₃H₇)₄, tetraethoxyorthosilicate (TEOS), Si(OC₂H₅)₄ and H₂O, respectively. Their droplets were carried to tubular assembly located in two consecutive electrically heated furnaces, where the reactants were evaporated and then mixed to react in vapor phase according to the mixing mode specified. Here, nebulizer-evaporator combination was used instead of temperature-controlled bubbling evaporator in order to keep all the reactants in vapor phase, avoiding their recondensation. Flow rate of the nitrogen gas through each nebulizer was 2×10^{-3} m³/min. Spray rates were 5.56×10^{-4} , 5.53×10^{-4} and 3.24×10^{-1} mol/min for TTIP, TEOS and H₂O, respectively. Almost equimolar TTIP and TEOS entered simply to get information of relative reactivity of the two precursors and eliminate effect of precursor ratio on particle properties. The spray rate of H₂O was highly excessive to react with the two alkoxides so as to maximize chance of the hy-

TABLE I Reactant introduced to each inlet port in Fig. 2 for the given method of mixing

Inlet port	Configuration		
	T-S	S-T	T/S
A	H ₂ O	H ₂ O	H ₂ O
B	TTIP	TEOS	
C			TTIP
D	TEOS	TTIP	TEOS

drolisis with respect to the thermal decomposition and eliminate effect of H₂O concentration on the hydrolyses and the successive particle formation.

The whole tubular assembly was made of quartz, whose configuration and dimension are shown in Fig. 2. In order to prepare various forms of composite TiO₂-SiO₂ particles, the reactants, TTIP, TEOS and H₂O were introduced and mixed in three different modes as indicated in Table I. For TiO₂(core)-SiO₂(shell) particles (abbreviated by T-S), H₂O and TTIP droplets were introduced to the innermost tube (A) and inner annular space (B), respectively, and heated to completely evaporate until their corresponding vapors met each other at the first mixing junction. TEOS droplets entered outer annular space (C, D) to evaporate by heating and then TEOS vapor finally met with product stream of reaction between TTIP and H₂O at the second junction of mixing. For SiO₂(core)-TiO₂(shell) particles (abbreviated by S-T), the entrances for TTIP and TEOS droplets were so interchanged that TEOS and TTIP met H₂O at the first and the second junctions, respectively. Each mixing junction was located in the middle of each electrical furnace. The mixing junctions were made by tapering the tube ends to enhance chance of mixing. This was very critical since the hydrolysis reaction of TTIP was so fast [9, 18] that mixing of the reactants could control its rate. On the other hand, for TiO₂-SiO₂ mixed particles (abbreviated by T/S), H₂O again entered through A, and TTIP and TEOS were introduced through C and D, respectively, with B closed. The two alkoxides were vaporized and mixed until they met with H₂O vapor coming out of the innermost tube at the second junction. Temperatures set by the two furnaces were the same and varied from 350°C to 950°C with

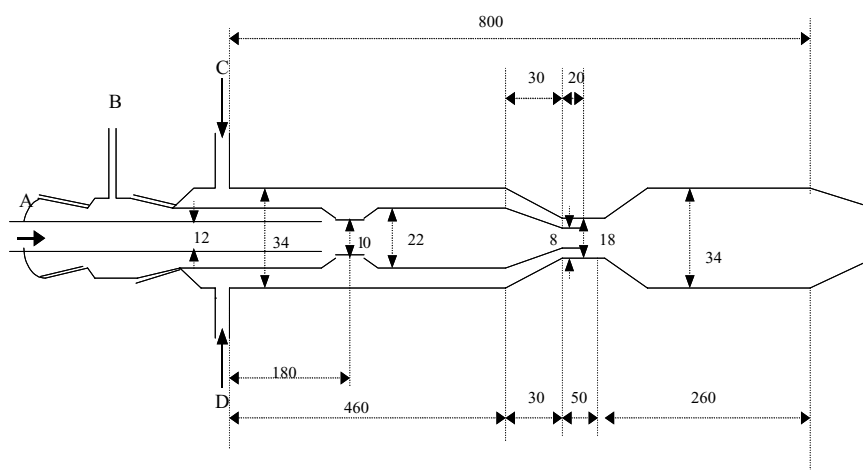


Figure 2 Reactor dimension in detail.

interval of 100°C. Under actual flow condition axial temperature distributions inside quartz tube were measured at 350°C and 850°C, respectively, to confirm that each set temperature was maintained in the zone corresponding to at least the middle 1/3 of each furnace axis. The gap between the two furnaces was made as short as possible to keep temperature drop there from the set temperature within 50°C. In the temperature range we used, the hydrolysis reaction was always expected to play an important role but the thermal decomposition would not be excluded as the temperature increased, as indicated by Kirkbir *et al.* [9].

Particles produced from the reactor were collected by air filter. The filtered particles were observed with Transmission Electron Microscope (EM912 Omega, Carl Zeiss). Size of the primary particles was obtained by measuring and averaging diameters of at least 100 particles in TEM images of each sample. Bulk chemical composition was measured with Energy Dispersive X-ray Spectrophotometer. Chemical bonds in the particles were identified by Fourier-Transform Infrared Spectroscopy (FT-IR, Perkin Elmer FT-IR 1615). Surface compositions of the particles were analyzed with pelletized particle samples by Auger Electron Spectroscopy (SAM4300, Perkin Elmer) at 5 KeV. X-ray Diffractometer (XRD, SDS2000, Scintag) was used to elucidate crystalline structures of the particles and Thermogravimetric Analyzer (TGA2050, TA Instrument) gave information on their thermal stability.

Results and discussion

Chemical compositions and structures of particles

Fig. 3 shows bulk silicon contents of the particles prepared with the various mixing methods as a function of reactor set temperature. Although TTIP and TEOS were introduced in equimolar amount with excess moles of H₂O, atomic percentages of silicon in all the particles were always less than 50% as shown in the figure. This

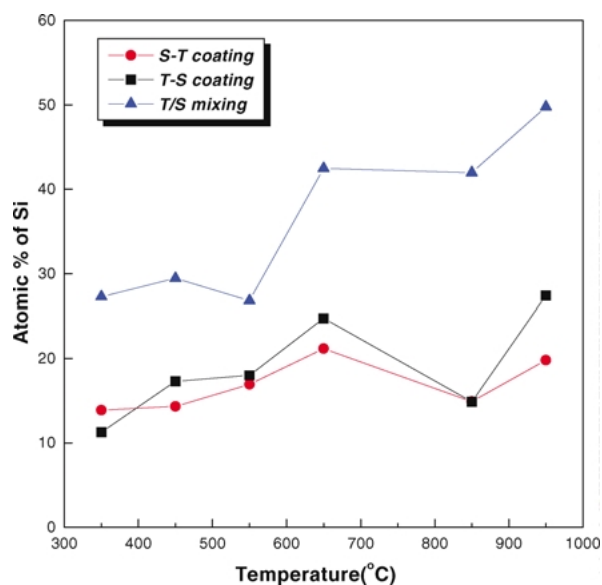


Figure 3 Effect of reactor set temperature on silicon content of the particles.

is explained by relative reactivity of TTIP to TEOS. Rate of TTIP hydrolysis is known so high [18] that the conversion of TTIP hydrolysis is 100% at as low as 200°C [9]. Even though few have been known quantitatively about rate of TEOS hydrolysis, TTIP and TiCl₄ are in general much more reactive than corresponding silicon compounds for thermal decomposition [19], oxidation [12, 13, 20] and hydrolysis [17], respectively. Under all our conditions, therefore, complete conversions were expected for TTIP while TEOS reacts short of completion such that the atomic percentage of silicon would not exceed 50%. On the other hand, it has been reported that the reactions of TEOS are catalyzed on free surface of TiO₂ [13, 17]. As shown in the figure, at the given temperature, T/S particles always have the highest silicon content of the three. In the T/S mode, TTIP and TEOS have comparable chance to react with H₂O but, due to higher reactivity of TTIP, large number of tiny TiO₂ nuclei would form prior to appreciable reaction of TEOS. Therefore, TEOS in this mode would find the largest surface area to react on, resulting in its highest conversion. Such single TiO₂ crystallites surrounded by thin layers of amorphous SiO₂ would then coagulate or coalesce to form the mixed-type T/S particles, as indicated by Suyama *et al.* [13]. In case of S-T mode, TEOS would have to convert to SiO₂, without any free surface of TiO₂. Thus, due to very slow rate of uncatalyzed hydrolysis, the S-T particles had the lowest content of silicon. In T-S mode, large number of small TiO₂ nuclei would be first produced in the same pattern as in the T/S mode. Since the nuclei, however, subsequently grow by coagulation, exposed surface of TiO₂ for TEOS appearing at the second mixing junction would be substantially reduced. Therefore, the silicon content of the particles would be much lower than that of T/S mode. However, since in spite of the coagulation there is some free surface of TiO₂ for the first layer of SiO₂ to be formed, the silicon content of the T-S mode is slightly higher than that of the S-T mode, as shown in the figure.

Due to Arrhenius effect, the silicon content of the particles from each mixing mode increased with the temperature. For the T/S particles prepared at 950°C, the atomic percentage of silicon approaches 50%, the same as the precursor composition, to indicate 100% conversion of TEOS. As noted in the figure, the temperature dependence of the silicon content is less appreciable in the T-S and the S-T than in the T/S since formation reactions of SiO₂ for the first two particles were less catalytic. This also supports the discussion on the role of TiO₂ surface exposed and the intraparticle structure of the particles.

Table II shows surface compositions of the three-mode particles prepared at 950°C with their corresponding bulk compositions. We made five measurements for each-mode particles. The silicon contents of the T-S and the T/S particles were much higher in their surfaces than either in their corresponding bulks or in their precursor mixtures (50%). As expected from our postulate on the intraparticle structures, the surface silicon content of the T-S was higher than that of the T/S while the opposite was true in bulk composition. It is

TABLE II Surface composition of various composite particles prepared at 950°C, otherwise under reference condition

Intraparticle structure	Atomic (%)	Ti	Si
T-S	Surface	11.1 ± 2.2	88.9 ± 1.8
	Bulk	72.6	27.4
S-T	Surface	100	Not detectable
	Bulk	80.2	19.8
T/S	Surface	19.9 ± 1.0	80.1 ± 0.9
	Bulk	50.2	49.8

very interesting that even the T/S particles have higher silicon content in their surface than in their bulk, which thus implies existence of radial composition gradient inside each primary particle. As described above, four steps would be involved to produce the final form of the T/S particles: reaction of TTIP, nucleation of TiO₂, surface reaction of TEOS on TiO₂ nuclei and coagulation of the coated nuclei. If the third and fourth steps occurred in series without overlapping, the T/S particles had no such a gradient, showing ideal mixedness.

Instead, the appearance of the composition gradient reflects actual overlapping of the last two steps. On the other hand, the T-S particles seem to have significant amount of core component in their surface in contrast to the S-T particles. This will be discussed in the next subsection.

Shapes and size of primary particles

Fig. 4 shows SEM pictures of the particles prepared by varying reactor set temperature under each mode of mixing. The primary particles were all isotropic and consisted of chain aggregates. Some particles prepared at 350°C are larger and more spherical than the others. These particles were probably produced by droplet-to-particle conversion due to incomplete evaporation of precursor droplets. As described above, the hydrolysis of TTIP occurs as low as 110°C, which is quite below boiling point of TTIP, there would be high possibility that the reactions precede the evaporation of the droplets. This will be further discussed in the next subsection. As the temperature increased above 350°C, size distribution of the primary particles gets narrow

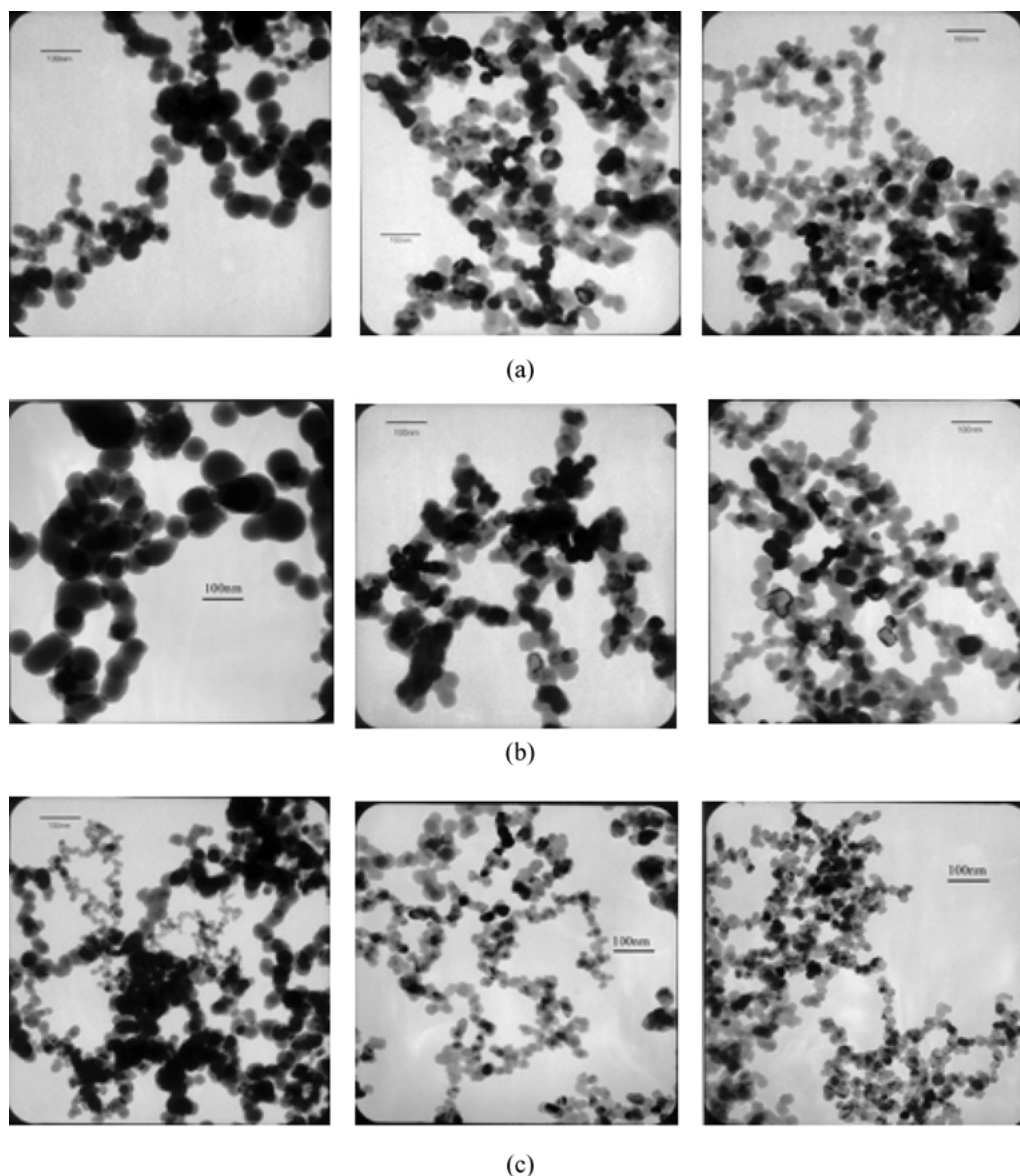


Figure 4 TEM images of various structures of composite particles prepared at 350, 650 and 950°C (from left to right). (a) T-S, (b) S-T and (c) T/S.

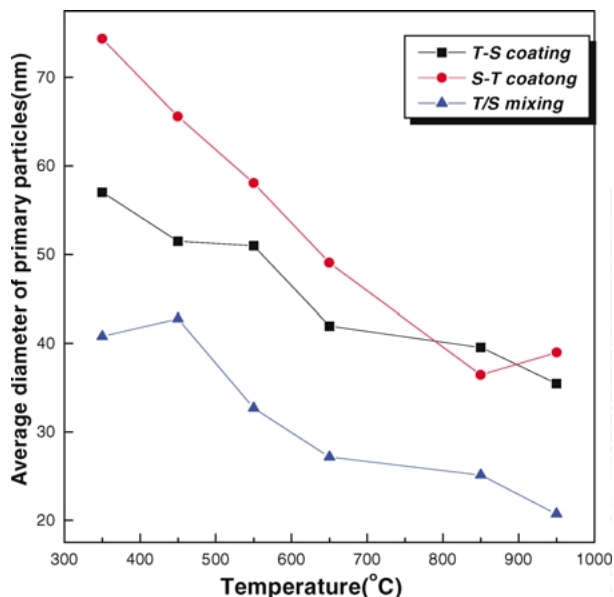


Figure 5 Effect of reactor set temperature on average of primary particles.

with geometric standard deviation no more than 1.27, and their average size ranges from 20 nm to 75 nm, depending on the mode of mixing and the reactor set temperature. As shown in Fig. 5 quantitatively, the primary particle size decreases with the temperature in each mode of reactant mixing and also decreases in order of S-T, T-S and T/S at the reactor set temperature given. These effects of the temperature and the mix-

ing mode on the primary particle size are opposite to their effect on the silicon content. As described before, the inclusion of Si^{+4} ions in the interstitial space of TiO_2 matrix inhibits the growth of the particles as well as the crystallization of TiO_2 phase. This phenomenon would be most pronounced in the T/S structure having the highest degree of SiO_2 dispersion inside each primary particle. In spite of the small difference in the silicon contents of the T-S and the S-T particles, however, the average sizes of the latter are significantly larger than the formers, except at high temperatures, where the reactivity of TEOS approaches that of TTIP. The significant difference is explained by different growth conditions imposed on the two particles. In the S-T mode, large but very few nuclei would be formed by SiO_2 molecules produced very slowly at the first junction. The number of nuclei would be too few to grow by coagulation. Therefore the nuclei themselves would be cores of the S-T particles. TiO_2 molecules produced at the second junction would condense on the SiO_2 cores rather than form their own nuclei. Due to such small number of the cores, the TiO_2 shell condensed would be thick. Thus the large core with the thick shell would give the S-T particles the largest of the three. Unreacted TEOS would have little chance in downstream of the second junction since these TiO_2 processes occurred immediately and ultimate area of TiO_2 free surface was very small. On the other hand, in case of the T-S particles, due to higher rate of TiO_2 nucleation caused by higher rate of TTIP reaction, the cores of the particles, in spite of coagulation, have smaller size but higher total

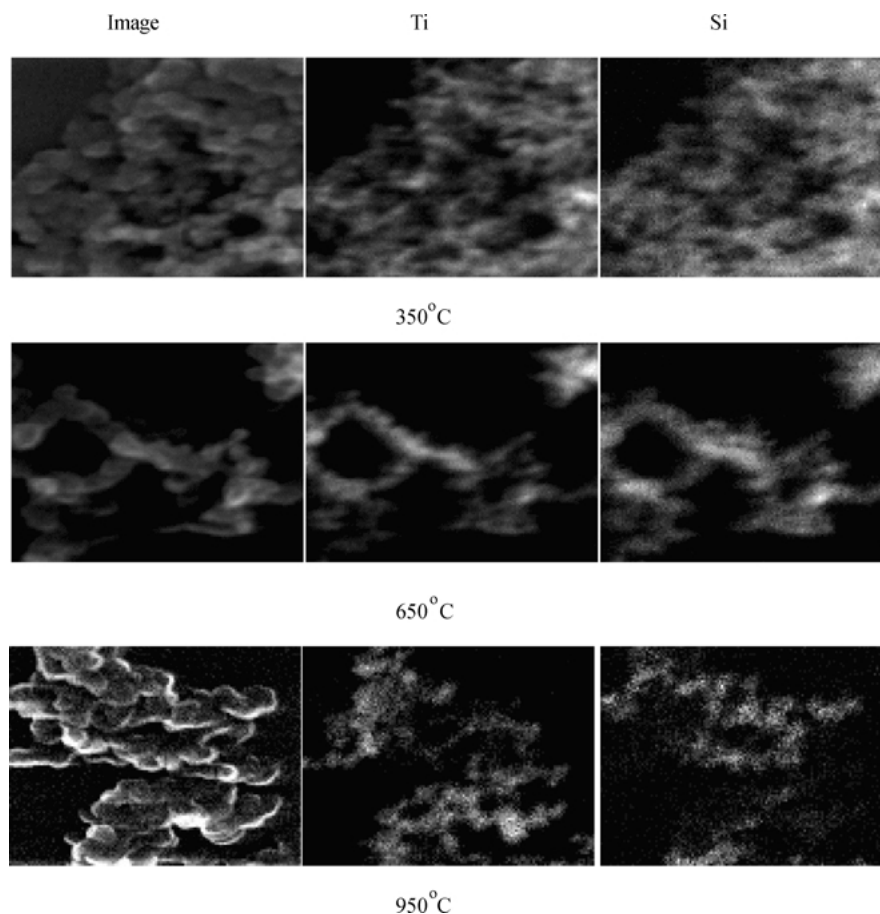


Figure 6 Ti/Si mapping of T/S particles prepared at different reactor temperatures.

surface area than those of the S-T particles. In addition, due to less reactive TEOS, the shells of the T-S particles would be so thin that the resulting T-S particles are the smaller than S-T particles. Furthermore, the thinness of the core of the T-S particles would make it possible that Auger electrons come from TiO_2 core as well as SiO_2 shell. However, no electrons in the core of the S-T particles could penetrate the thick TiO_2 shell. This also explains both the promoted difference in the primary particle size between the two particles and the appearance of core component in the surface composition of the T-S particles.

Thermogravimetry, FT-IR and crystallinity

All the samples prepared above 450°C had gray-colored appearances, originating from incomplete thermal decomposition of alcohol groups in the alkoxides, which darkened with the reactor set temperature. Two T-S particles prepared at 950 and 350°C , respectively, were analyzed thermogravimetrically under air environment. The carbonaceous materials in the former particles disappeared with color change to white between 200 to 400°C with weight loss of 4% . No additional change in weight was observed up to 1000°C . However, the latter sample, even though it had no carbonaceous materials, lost as high as 12% of its original weight up to 300°C . Thus, it is supposed that the particles prepared at 350°C contained some metal alkoxides or their intermediates to be further decomposed to the oxide, probably by droplet-to-particle conversion, as described in the previous subsection.

The components of Ti and Si were mapped from the SEM images for the T/S particles prepared at 350 , 650 and 950°C , respectively, as shown in Fig. 6. Except 950°C sample, each image and the corresponding two mappings are all coincided, implying that the components are well dispersed in both intra- and interparticle senses. The coincidence, however, fails for 950°C sample. This suggests that the increase in the temperature causes segregation of the components from particle to particle probably by self-nucleation of SiO_2 .

Fig. 7a and b shows FT-IR analyses of the three-mode samples prepared at 950°C and the T/S particles obtained at three different temperatures, respectively. As shown in Fig. 7a, the T/S sample is the only one to possess Ti—O—Si band at 975 cm^{-1} . Furthermore, Fig. 7b shows all the T/S particles have the bands whose depths and frequencies keep unchanged with the temperatures between 350 and 950°C . The bands representing Ti—O bond in Fig. 7a for the S-T, the T-S and the T/S particles prepared at 950°C were located at 669 , 669 and 667 cm^{-1} , respectively, showing little shift between the samples. This indicates that TiO_2 has already formed the same crystalline structure for all the samples. Fig. 7b, however, shows that the bands of the T/S samples significantly move to lower frequency as the temperature decreases: They are 667 , 657 and 632 cm^{-1} for the 950 -, 650 - and 350°C -samples, respectively, implying the TiO_2 phase varied with the temperature. On the other hand, location of band around 1100 cm^{-1} spe-

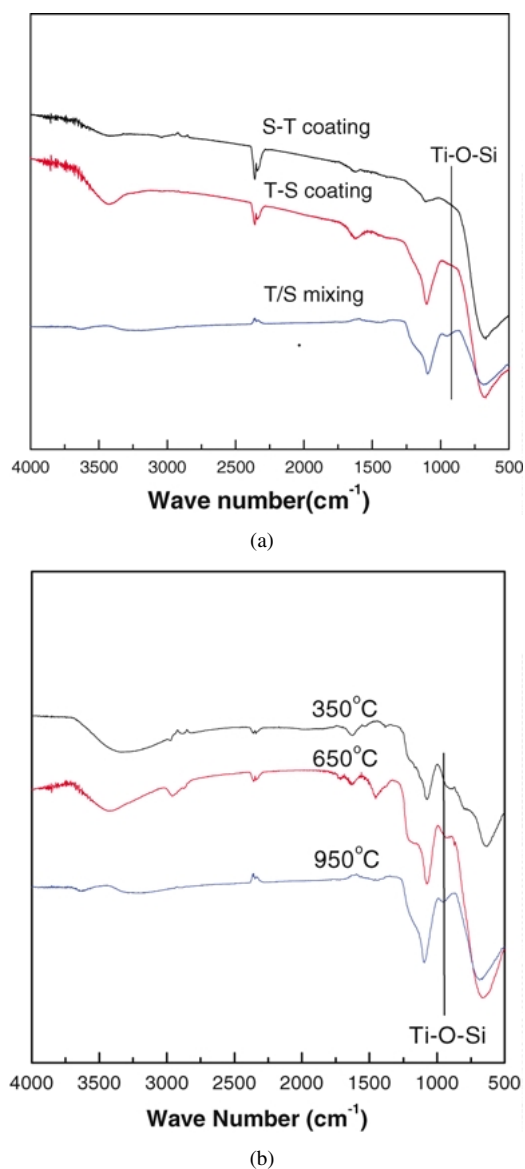


Figure 7 FT-IR spectra of various particles. (a) Particles prepared at 950°C with different structures, and (b) T/S particles prepared at different reactor temperatures.

cific to Si—O asymmetric stretching bond slightly shifts according to the mixing modes as well as the reactor set temperature. In Fig. 7a, the bands appear at 1110 cm^{-1} , 1103 and 1095 cm^{-1} for the S-T, T-S and T/S particles, respectively. In Fig. 7b they locate at 1095 , 1076 and 1074 cm^{-1} for the T/S particles prepared at 950 , 650 and 350°C , respectively. It is thus proposed that the shifts in the location of the Si—O band were related with segregation of the components: For SiO_2 , maximum degree of segregation would be obtained in cores of the S-T particles while SiO_2 phase of the T/S particles is least segregated. However, for the T-S particles, SiO_2 shell phase would be not in complete segregation but in intermediate one by influence of core phase, as described later. Effect of the temperature on the shift would also be related with the segregation of the Si component, as shown in Fig. 6. Jiwei *et al.* [21] also pointed out similar trend in TiO_2 - SiO_2 composite film prepared from sol-gel processing.

XRD analyses show that TiO_2 phases in all types of the composite particles were transformed from

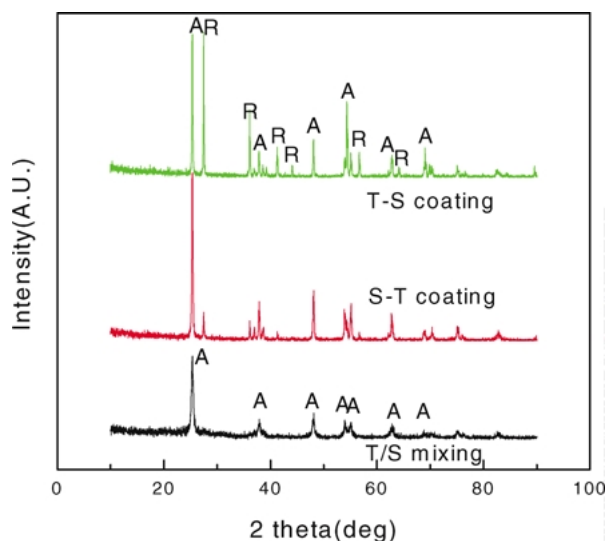


Figure 8 XRD patterns of 550°C-particles sintered at 800°C.

amorphous to anatase at the reactor set temperatures between 450 and 550°C. No rutile peaks appeared up to 950°C probably due to short residence time in the reactor. The crystallization temperature was about 100°C, one temperature interval higher than that of pure TiO₂ particles, showing the retardation effect of the silicon component on the crystallization. In XRD patterns, peak heights of anatase were reduced accordingly with the silicon content of the composite particles. When the three-mode particles prepared at 550°C were heat-treated at 800°C for 30 min, respectively, interesting results were obtained as shown in Fig. 8. The T/S particles, even after the heat treatment, still remained in anatase while the T-S and the S-T particles exhibit some rutile peaks. It is confirmed that least segregated T/S particles have the highest retardation effect of SiO₂ on their transformation to rutile while the segregated structures such as the T-S and the S-T forms were relatively free to transform to rutile. TiO₂ in the T-S particles was more transformable than that in the S-T particles, as shown in the figure. It is supposed that TiO₂ in the cores of the T-S particles had less limitation in the transformation because the core structure was formed prior to amorphous shell of SiO₂. On the other hand, since TiO₂ in the shells of the S-T particles was structured on the SiO₂ core surface, the core would affect TiO₂ phase. Similarly, SiO₂ shell of the T-S particles would be influenced by structure of TiO₂ core.

Conclusion

Various composite structures such as TiO₂-SiO₂ mixed, TiO₂(core)-SiO₂(shell) and SiO₂(core)-TiO₂(shell) have been prepared by vapor-phase hydrolysis of the corresponding alkoxides. Since reaction of TTIP was so fast that design of mixing junction was very important. Hydrolysis rate of TEOS was, however, much

lower than that of TTIP, catalyzed on free surface of TiO₂. Therefore, atomic percentages of silicon in the particles were always less than 50% and increased with availability of TiO₂ surface, such as S-T, T-S and T/S in order, as well as reactor set temperature. For the T/S particles prepared at 950°C, the atomic silicon % reached 50%, meaning complete conversion of TEOS, and SiO₂-rich particles appeared by self nucleation of SiO₂. Average size of primary particles decreased with their silicon content. Nucleation rate determined by the rate of hydrolysis more pronounced the difference in the primary particle size between T-S and S-T particles. The T/S particles with the highest mixedness, however, had a gradient of composition in radial direction. Structural identity of shell component was limited by the existence of core component for both the T-S and the S-T particles.

References

1. A. J. RULISON, P. F. MIQUEL and J. L. KATZ, *J. Mater. Res.* **11** (1996) 3083.
2. M. K. AKHTAR, Y. XIONG and S. E. PRATSINIS, *AIChE J.* **7** (1991) 1561.
3. M. K. AKHTAR, S. VEMURY and S. E. PRATSINIS, *ibid.* **40** (1994) 1183.
4. H. D. JANG, *Ceram. Processing* **43** (1997) 2704.
5. S. E. PRATSINIS and P. T. SPICER, *Chem. Eng. Sci.* **53** (1998) 1861.
6. H. KOMIYAMA, T. KANAI and H. INOUE, *Chem. Lett.* (1984) 1283.
7. F. KIRKBIR and H. KOMIYAMA, *The Can. J. Chem. Eng.* **65** (1987) 759.
8. K. M. S. KHALIL, M. I. ZAKI and A. A. EL-SAMAHY, *J. Anal. & Appl. Pyrol.* **42** (1997) 123.
9. F. KIRKBIR and H. KOMIYAMA, *Chem. Lett.* (1988) 791.
10. Q. H. POWELL, G. P. FOTOU, T. T. KODAS and B. ANDERSON, *J. Aerosol Sci.* **26** (1995) S557.
11. S. JAIN, T. T. KODAS, M. K. WU and P. PRESTON, *ibid.* **28** (1997) 133.
12. S. H. EHRMAN, S. K. FRIEDLANDER and M. R. ZACHARIAH, *ibid.* **29** (1998) 687.
13. Y. SUYAMA, E. URA and A. KATO, *Jap. J. Chem. Soc. (Japan)* (1978) 356.
14. M. K. AKHTAR, S. PRATSINIS and S. V. R. MASTRANGELO, *J. Am. Ceram. Soc.* **75** (1992) 3408.
15. G. P. FOTOU, T. T. KODAS and B. ANDERSON, *Aerosol Sci. Technol.* **33** (2000) 557.
16. C. ANDERSON and A. J. BARD, *J. Phys. Chem.* **99** (1995) 9882.
17. S. K. LEE, K. W. CHUNG and S.-G. KIM, *Aerosol Sci. Technol.* **36** (2002) 763.
18. B. J. INGEBRETHSEN, E. MATIJEVIC and R. E. PARTCH, *J. Colloid Interf. Sci.* **95** (1983) 228.
19. K. OKUYAMA, Y. KOUSAKA, N. TOHGE, S. YAMAMOTO, J. J. WU, FLAGEN and J. H. SEINFELD, *AIChE J.* **32** (1986) 2010.
20. Y. XIONG, M. K. AKHTAR and S. E. PRATSINIS, *J. Aerosol Sci.* **24** (1993) 301.
21. Z. JIWEI, Y. TAO, Z. LIANGYING and Y. XI, *Ceram. Intern.* **25** (1999) 667.

Received 20 August 2002

and accepted 17 March 2003